Ink-Jet Printability for Fluids

Daehwan Jang*, Dongjo Kim and Jooho Moon
Dept. of Materials Science and Engineering, Yonsei University, Seoul, Korea
Phone:+82-2-2123-2855, E-mail: myelysion@yonsei.ac.kr

Keywords : Ink-jet printing, printability, droplet formation dynamics

Abstract

We have investigated the inter-relationship between the ink-jet printability and the physical fluid properties by monitoring the droplet formation dynamics. Printability of the fluids was judged based on the inverse of Ohnesorge number (Z^{-1}) that relates to the viscosity, surface tension, and density of the fluid.

1. Introduction

Ink-jet printing is an emerging technology, being explored extensively beyond image transfer capability, with many applications including microdispensing and materials assembly [1-5]. Recently it has been used to fabricate polymeric electroluminescent, controlled release drug delivery devices in pharmaceuticals, and refractive microlenses made of hybrid organic-inorganic materials [2]. The ink-jet printing method most commonly used for modern industrial applications is the drop-on-demand (DOD) that permits selective deposition of precise quantities of functional inks on arbitrary surface in the form of droplets by applying a short pressure pulse through a nozzle of typically 20-50 μm diameter [6].

However, the appropriate functional ink materials are limited. Inappropriate ink will lead to unstable ink-jetting in which long-lived filaments form, connecting the ejected droplet with the nozzle [7]. Length and life time of the filament influence considerably the positional accuracy and resolution of the printing as well as the printability of the inks. In order to be printed, it is necessary for the fluids to have adequate physical properties. The fluid dynamics of DOD ink-jet printing have been studied [8-10]. The physical parameters of the fluid that are important in ink-jetting mechanism are viscosity, density, and surface tension. These properties of the fluid influence the drop formation mechanism and subsequent drop size at a given voltage. Fromm predicted based on a numerical analysis using complete incompressible flow equations that stable drop formation in DOD system is permitted only when $Z^{-1} > 2$ [11]. Later Reis and Derby further investigated that the printable fluid should have the Z^{-1} value between 1 and 10. They explored the influence of fluid properties on the ink-jet printing behavior using computational fluid dynamics that model the free surface flow characteristic of drop formation in conjunction with a parallel experimental study. They claimed that the lower limit is governed by fluid viscosity dissipating the pressure pulse, whereas the satellite forms instead of single droplet beyond the upper limit [12].

In this study, we redefine the printable range of the Z^{-1} by in-situ monitoring of droplet formation dynamics for various fluids having varying Z^{-1} values. We can determine the Z^{-1} range by considering practical aspects of the printing such as single droplet formability, minimum stand-off distance (i. e., the distance from nozzle tip to the substrate), positional accuracy, and maximum allowable jetting frequency. These can be used to reduce the number of experiments needed for the determination of optimal ink-jetting condition for each fluid.

2. Experimental

A mixture of distilled water and ethylene glycol (15, 25, 50, 75 mol%), a mixture of distilled water and diethylene glycol (50 mol%), and diethylene glycol were used in the experiment. The inverse Ohnesorge number varied from 1 to 17 for these mixed solvents. Viscosity and surface tension were measured using a Peltier concentric-cylinder double-gap rheometer (AR2000ex, TA Instruments Inc., UK) and tensiometer (DST30, SEO), respectively. The drop formation of fluid was captured using the CCD camera with an inter-frame time of 1μ equipped with a strobe LED light to view individual droplets and measure their size and travel velocity.

The printer set up consisted of a drop-on-demand (DOD) piezoelectric ink-jet nozzle manufactured from Microfab Technologies, Inc. (Plano, TX) and the diameter of orifice was 50 μm. Droplet formation of each fluid was performed by applying a 25V, 23-μs impulse at a frequency of 1000 Hz.

The CCD camera can snapshot the drop formation dynamics with an inter-frame time of 1 μs equipped with a strobe LED light to view individual droplets and measure their size and travel velocity. By increasing the delay times of the camera in the step of 1 μs, the drop dynamics was captured. Images of a droplet were taken at various delay time intervals and subsequently indicated the flight distance from the nozzle tip. The ink-jet printing was carried out in 40% relative humidity at 25 °C.

3. Results and discussion

Dynamics of fluid droplet formation as a function of the Z^{-1} values is visualized. The inverse of Ohnesorge numbers for the fluids shown in Figs. 1a, b, c, d and e are 2.17, 4.08, 6.57, 13.68, and 17.32, respectively. The delivered pressure pulse pushes the fluid out of the nozzle tip and the meniscus bulges quickly until a filament with a round head forms at the elapse time of 20 – 40 μs. Traveling velocity difference between droplet head and filament makes the droplet filament stretched until the elapse time reaches about 60 – 120 μs. During the stretching of the fluid filament, the tail of the fluid filament near the nozzle tip is continuously necking, forming a long fluid filament. The tail of the filament ruptures from the nozzle tip finally and recoils back to the drop head in order to minimize surface area for the fluids with the Z^{-1} in the range of 2 – 4. The filament length shrinks further and single droplet forms eventually at the elapse time of 160 – 200 μs (Fig. 1a and b). For the fluids with the Z^{-1} in the range of 6 – 13 (Fig. 1c and d), on the other hand, the recoiling filament is detached from the falling droplet, generating a primary droplet and a transient satellite, both of which merge together into single droplet at the elapse time of 140 –180 μs. In contrast, for the fluid with the Z^{-1} of 17.32, the satellite is unable to merge with the primary droplet even after 200 μs (Fig. 1e).

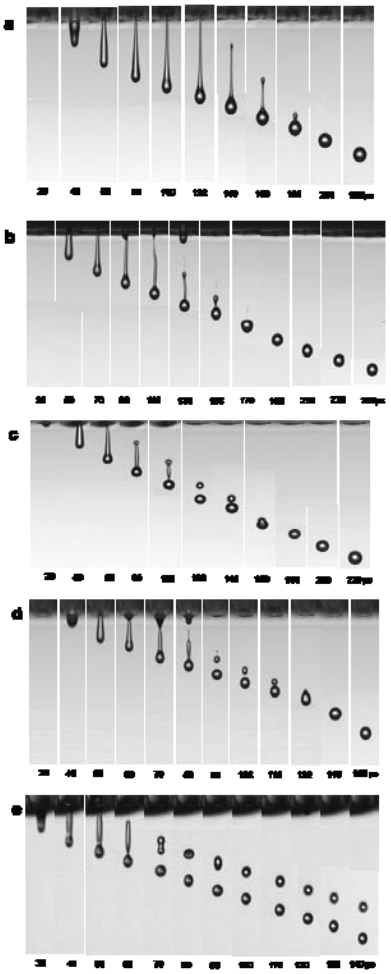

Fig. 1. Representative photo sequence of drop formation for the fluids with the Z^{-1} values in the range of 2 - 17 at a constant driving voltage of 25 V: (a) Z^{-1} = 2.17; (b) Z^{-1} = 4.08; (c) Z^{-1} = 6.57; (d) Z^{-1} = 13.68; and (e) Z^{-1} = 17.32.

Based on the in-situ monitoring, droplet formation process involves the successive events of ejection and stretching of the fluid, necking, rupture and recoil of the fluid, and formation and recombination of single droplet and satellite. For quantitative analysis of droplet formation behavior, the positions of several representative points on the ejected fluid are plotted versus the elapse time (Fig. 2). At the early stage, the black colored dots represent the head trajectory of the fluid ejected from the nozzle, which becomes the tip of the primary droplet at the later stage. The red colored dots indicate the rupture point of fluid apart from the nozzle, which represents the tail trajectory of fluid filament later. Time at which the filament ruptures from the nozzle is defined as a rupture time.

The moment at which the head and tail trajectories merge corresponds to the formation of single droplet. Such a graphical description divides the jetting process into three distinct stages: filament elongation, filament recoiling, and single droplet formation. Figure 2 enables us to compare the jetting behavior such as filament rupture time, filament length, and time for single droplet formation as a function of the Z^{-1}.

For the fluids with low Z^{-1} values in the range of 2 – 4 (Figs. 2a and b), a round protruding head of the filament forms at the elapse time of ~ 50 μs and the filament is stretched until the time of ~ 120 μs. Filament rupture occurs at the time of ~ 140 μs. In contrast, the fluids with medium Z^{-1} values in the range of 6 – 13 are subjected to faster filament elongation and earlier rupture as shown in Figs. 2c and d. The fluids bulges to form a round filament head at the time of ~ 40 μs and the filament elongation occurs until ~ 60 μs, which eventually ruptures at ~ 80 μs. The fluid with high Z^{-1} value above 14 experiences even rapid filament elongation and rupture as shown in Fig. 2e. Slope of the head trajectory represents the travel velocity of the falling droplet. Within a short travel distance of 1000 μm, we can assume that the falling microdroplets of small masses travel at the constant velocity ignoring the gravity-induced acceleration, even though the droplet size varies depending on the Z^{-1} value. The travel velocity of the droplet increases with increasing Z^{-1} value: 2.6 m/s when Z^{-1} = 2.17, 2.88 m/s when Z^{-1} = 4.08, 3.4 m/s when Z^{-1} = 6.57, 3.63 m/s when Z^{-1} = 13.68, and 3.63 m/s when Z^{-1} = 17.32, respectively. In contrast, the retreating velocity of the tail decreases with increasing Z^{-1} value determined by the slope of tail trajectory: 5.29 m/s when Z^{-1} = 2.17, 4.45 m/s when Z^{-1} = 4.08, 4.38 m/s when Z^{-1} = 6.57, 4.37 m/s when Z^{-1} = 13.68, and 3.16 m/s when Z^{-1} = 17.32, respectively. These opposite tendency makes the filament recoiling stage occurred within the duration of 70~90 μs, independent of the Z^{-1} values. The higher viscosity of the fluid is, the more energy viscously dissipated is, resulting in smaller kinetic energy available. As the value of Z^{-1} decreases, therefore, the travel velocity of the droplet head decreases mainly due to the increased viscosity.

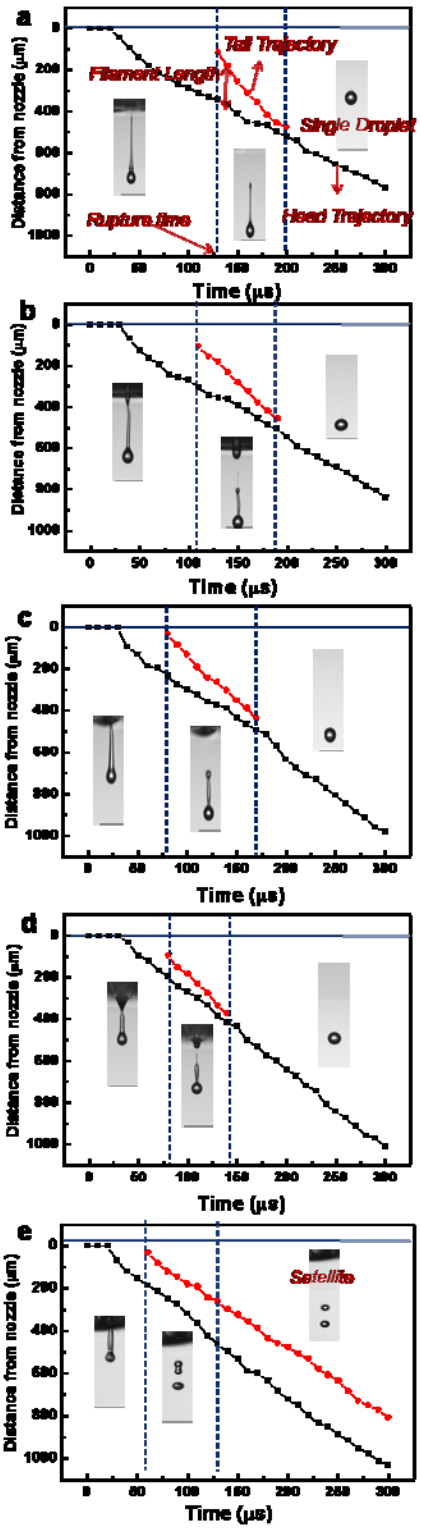

Fig. 2. Representative trajectories of the ejected droplets as a function of the elapse time for the fluids with the Z^{-1} values in the range of 2 - 17 at a constant driving

voltage of 25 V: (a) Z^{-1} = 2.17; (b) Z^{-1} = 4.08; (c) Z^{-1} = 6.57; (d) Z^{-1} = 13.68; and (e) Z^{-1} = 17.32.

Figure 3(a) shows the minimum stand-off distance (MSD) between the nozzle tip and the substrate required for printing of each fluid as a function of Z^{-1}. The flying distance where the fluid ejected from the nozzle transforms into a single droplet can define the minimum stand-off distance (MSD). The printing performed at the distance less than the MSD results in the deposition of droplets with tails and satellites, degrading the printing resolution. Figure 5a shows the variation of the minimum stand-off distance as a function of Z^{-1}. As the Z^{-1} decreases, the minimum stand-off distance for ink-jet printing increased. As the Z^{-1} decrease from 13.68 to 4.08, the MSD linearly increases from 436 μm to 541 μm under the given driving voltage, but it soars to 650 μm when $Z^{-1} < 4$. The ink-jet printing at longer MSD will lead to unstable and inaccurate deposition. The positioning error due to the variation in the stand-off distance was exhibited in Fig. 3(b). As the value of Z^{-1} decreases, the positioning error increases due to the formation of long filament and longer time required for single droplet formation. These studies demonstrate how the fluid properties can influence the ink-jet printability. Inappropriate properties of fluid with Z^{-1} less than 4 used in the ink-jet printing result in the formation of long-lived filaments and longer stand-off distance, and consequently large positioning error. In order to reduce the positioning error and increase the printability of fluid, we need to control dimensionless number, Z^{-1}, for better printability.

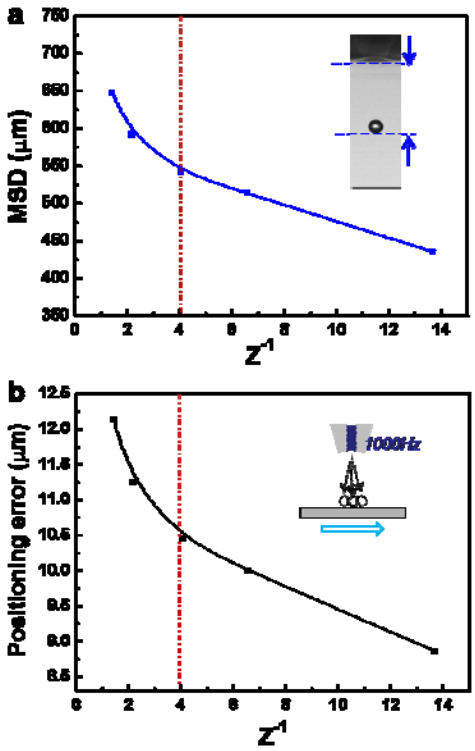

Fig. 3. (a) Variation of the minimum stand-off distance (MSD) as a function of Z^{-1}; (b) the calculated positioning error as a function of Z^{-1}

4. Summary

In our research, we have investigated the inter-relationship between the ink-jet printability and the physical fluid properties. By in-situ monitoring the jetting dynamics using an image system with an inter-frame time of 1μs, the droplet formation behavior was characterized in the term of the inverse (Z^{-1}) of Ohnesorge number that relates to the viscosity, surface tension, and density of the fluid. We have redefined the printable range as $4 \leq Z^{-1} \leq 14$ by considering practical aspects of the printing such as single droplet formability, minimum stand-off distance, positional accuracy, and maximum allowable jetting frequency. Printing the fluid with low Z^{-1} less than 4 results in larger sized droplet formation with a long-lived filament and takes longer time until single droplet generation, which in turn degrades the positional accuracy and the printing resolution.

5. References

1. B. Derby, N. Reis, *MRS Bull.*, 28, 815 (2003).
2. B. –J. Gans, P. C. Duineveld, U. S Schubert, *Adv. Mater.*, 16, 203 (2004).
3. S. Jeong, K. Woo, D. Kim, S. Lim, J. Kim, H. Shin, Y. Xia, J. Moon, *Adv. Funct. Mater.*, 18, 679 (2008).
4. S. Jeong, D. Kim, J. Moon, *J. Phys. Chem. C*, 14, 5245 (2008).
5. D. Kim, S. Jeong, B. Park, J. Moon, *Appl. Phys. Lett*., 89, 264101 1 (2006).
6. H. P. Le, *J. Imaging Sci. Technol*., 42. 49 (1998).
7. B.-J. Gans, E. Kazancioglu, W. Meyer, U. S. Schubert, *Macromol. Rapid Commun*., 25, 292 (2004).
8. H. Dong, W. W. Carr, J. F. Morris, *Phys. Fluids*, 18, 072102 1 (2006).
9. Q. Xu, O. A. Basaran, *Phys. Fluids*, 19, 102111 1 (2007).
10. X. Zhang, O. A. Basaran, *Phys. Fluids*, 6, 1184 (1995).
11. J. E. Fromm, *IBM J. Res. Dev*., 28, 322 (1984).
12. N, Reis, B. Derby, *Mater. Res. Soc. Symp. Proc*., 625, 117 (2000).